



## The Cantabrian capercaillie: A population on the edge

José Jiménez<sup>a,\*</sup>, Raquel Godinho<sup>b,c,d,1</sup>, Daniel Pinto<sup>e</sup>, Susana Lopes<sup>b,d</sup>, Diana Castro<sup>b,d</sup>, David Cubero<sup>f</sup>, M. Angeles Osorio<sup>g</sup>, Josep Piqué<sup>h</sup>, Rubén Moreno-Opo<sup>i</sup>, Pablo Quiros<sup>j</sup>, Daniel González-Nuevo<sup>j</sup>, Orencio Hernandez-Palacios<sup>j</sup>, Marc Kéry<sup>k</sup>

<sup>a</sup> Instituto de Investigación en Recursos Cinegéticos (IREC, CSIC-UCLM-JCCM), Ronda de Toledo 12, 13071 Ciudad Real, Spain

<sup>b</sup> CIBIO, Centro de Investigação em Biodiversidade e Recursos Genéticos, InBIO Laboratório Associado, Universidade do Porto, Campus de Vairão, 4485-661 Vairão, Portugal

<sup>c</sup> Departamento de Biología, Faculdade de Ciências, Universidade do Porto, 4169-007 Porto, Portugal

<sup>d</sup> BIOPOLIS Program in Genomics, Biodiversity and Land Planning, CIBIO, Campus de Vairão, 4485-661 Vairão, Portugal

<sup>e</sup> Fundación Patrimonio Natural de Castilla y León, Cañada Real 306, Edificio Prae, 47007 Valladolid, Spain

<sup>f</sup> Dirección General de Patrimonio Natural y Política Forestal, Junta de Castilla y León, c/Rigoberto Cortejoso 14, 47014 Valladolid, Spain

<sup>g</sup> Servicio Territorial de Medio Ambiente de León, Avda. Peregrinos, s/n, 24071 León, Spain

<sup>h</sup> Tragsatec, c/Julián Camarillo 6B, 28037 Madrid, Spain

<sup>i</sup> Subdirección General de Biodiversidad Terrestre y Marina, Ministerio para la Transición Ecológica y el Reto Demográfico, Pza. San Juan de la Cruz 10, 28071 Madrid, Spain

<sup>j</sup> Dirección General de Medio Natural, Principado de Asturias, c/Trece Rosas, 2, 33005 Oviedo, Spain

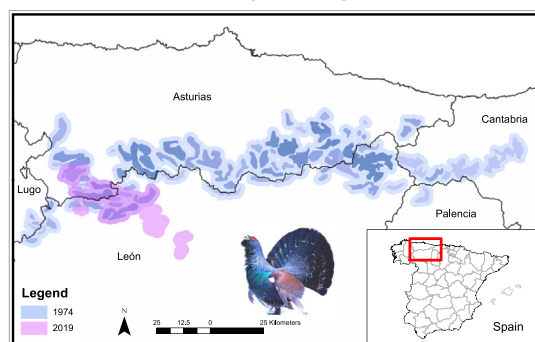
<sup>k</sup> Swiss Ornithological Institute, Sempach, Switzerland

### HIGHLIGHTS

- Cantabrian capercaillie population has recently been classified as "Critically Endangered" by Spanish Government.
- To develop management plans, information on demographic parameters are necessary to understand population dynamics.
- In 2019 we estimated the size of population at 191 individuals.
- Since the 1970s, we estimated a shrinkage of the population range by 83%.
- Apparent annual survival was estimated at 0.707 and per-capita recruitment at 0.233.

### GRAPHICAL ABSTRACT

Distribution map for the 1970's (from Castroviejo et al., 1974) and current range of the Cantabrian capercaillie. In the inset, location of the study area in Spain.



### ARTICLE INFO

#### Article history:

Received 5 November 2021

Received in revised form 11 January 2022

Accepted 25 January 2022

Available online 29 January 2022

Editor: Rafael Mateo Soria

#### Keywords:

Capercaillie

Dail-Madsen model

### ABSTRACT

The capercaillie *Tetrao urogallus* - the world's largest grouse- is a circumboreal forest species, which only two remaining populations in Spain: one in the Cantabrian mountains in the west and the other in the Pyrenees further east. Both have shown severe declines, especially in the Cantabrian population, which has recently been classified as "Critically Endangered". To develop management plans, information on demographic parameters is necessary to understand and forecast population dynamics. We used spatial capture-recapture (SCR) modeling and non-invasive DNA samples to estimate the current population size in the whole Cantabrian mountain range. In addition, for the assessment of population status, we analyzed the population trajectory over the last 42 years (1978–2019) at 196 leks on the Southern slope of the range, using an integrated population model with a Dail-Madsen model at its core, combined with a multistate capture-recapture model for survival and a Poisson regression for productivity. For 2019, we estimate the size of the entire population at 191 individuals (95% BCI 165–222) for an estimated 60 (48–78) females and 131 (109–157)

\* Corresponding author.

E-mail address: [Jose.Jimenez@uclm.es](mailto:Jose.Jimenez@uclm.es) (J. Jiménez).

<sup>1</sup> Equal contribution.

Integrated population model (IPM)  
 Population size  
 Recruitment  
 Spatial capture-recapture (SCR)  
 Survival

males. Since the 1970s, our study estimates a shrinkage of the population range by 83%. The population at the studied leks in 2019 was at about 10% of the size estimated for 1978. Apparent annual survival was estimated at 0.707 (0.677–0.735), and per-capita recruitment at 0.233 (0.207–0.262), and insufficient to maintain a stable population. We suggest work to improve the recruitment (and survival) and manage these mountain forests for capercaillie conservation. Also, in the future, management should assess the genetic viability of this population.

## 1. Introduction

The Western capercaillie *Tetrao urogallus* is a boreal species that typically inhabits mountainous forests in the West, Northwest and central Palearctic region. Eight subspecies are currently recognized, including a Cantabrian subspecies *T. u. cantabricus* (de Juana and Kirwan, 2020). Although some genetic studies have supported its validity (Rodríguez-Muñoz et al., 2007), others have suggested that the Cantabrian and Pyrenean (*T. u. aquitanicus*) populations belong to the same evolutionary unit (Duriez et al., 2007; Leclercq and Menoni, 2018). Whereas the capercaillie as a species is considered to have a “Least Concern” Red List threat status for Europe as a whole (BirdLife International, 2021), the Cantabrian population's conservation status was assessed as “Endangered C1; C2a(i)” by Storch et al. (2006) for the IUCN. In 2018 it was declared “Critically Endangered” by the Spanish Government (Ministerio para la Transición Ecológica, 2018).

Our objective was to understand the status, population trends, and the demographic drivers governing the population dynamics of Cantabrian capercaillie. Currently the Spanish government and regional authorities are implementing several management actions that deserve to be assessed to check their effectiveness. This analysis also constitutes a tool to monitor and predict the effect of specific, ongoing conservation efforts and, in the light of our results, propose alternative future management. Accordingly, we conducted three separate analyses: 1) we estimate the current population size for the whole of the Cantabrian mountains, 2) we compare the current range of the Cantabrian capercaillie with its range as documented in the 1970s by Castroviejo et al. (1974), and 3) we assess the population trajectory of the Cantabrian capercaillie using a demographic model and thereby also obtain precise estimates of key demographic parameters for the population growth (annual survival, recruitment and immigration-emigration).

### 1.1. Population size

Capercaillie have a lek-based mating system, where males display over a limited area (called a lek or “cantadero” in Spanish) to attract females (Storch, 1997). Because of this characteristic aggregation in leks, monitoring of this species for the assessment of population size and trends has typically been based on counts at leks (Pollo et al., 2003), productivity sampling at the end of the breeding period (Benito, 2019), and recently capture-recapture and genotype-based methods deployed at leks (Morán-Luis et al., 2014; Pérez et al., 2011). Population size estimation using non-spatial capture-recapture (CR) methods is a standard approach in wildlife research (Williams et al., 2002) but there are some challenges, such a negative bias induced in population size estimates by unmodelled individual heterogeneity in capture probability (Karanth and Nichols, 1998) due to the spatial organization of individuals relative to traps (Royle et al., 2014). This problem has been overcome with spatial capture-recapture (SCR) models (Borchers and Efford, 2008; Efford et al., 2004; Royle et al., 2009). SCR has previously been used for capercaillie population estimates (Augustine et al., 2020; Mollet et al., 2015) using non-invasive monitoring based on DNA obtained from feces. These authors also showed how the population size in any sub-area can be readily estimated by tallying up the number of estimated activity centers in each. In addition, it is worth noting that working with explicit spatial information may help accounting for trap-specific variability. We decided to use the same approach (DNA monitoring + SCR model) to estimate population sizes as did these authors.

### 1.2. Change in distributional range

To assess the change in the distributional range, we compared the distribution in the 1970s (Castroviejo et al., 1974) with the current one.

### 1.3. Population trajectory

The assessment of the population trajectory was a more challenging task. Lek count monitoring merely produces an index of population size, which depends on abundance, but also on the probability of detection (including lek-attendance probability) of the birds (Hostetter et al., 2019; Péron and Garel, 2019), and imperfect and variable detectability is an important potential source of bias in any wildlife study (Kellner and Swihart, 2014). We decided to restrict our analyses to the use of lek count data from just a part of the whole range distribution; the Southern slope of the mountain range described by Pollo et al. (2005) -which comprised 40–50% of the population in the 1990s- because in that area data were available for the entire period, rather than only for part of the years as in the rest of the range. These lek data were collected by field biologist and forest rangers between 1978 and 2019. For inference about demographics based on this data, we adopted the Dail-Madsen (DM) model (Dail and Madsen, 2011) which uses replicate count data of unidentified animals at multiple sites, allowing abundance to be estimated while correcting for imperfect detection probability. This model is an extension of the binomial mixture model of Royle (2004) to include population dynamics, where annual abundances in subsequent years are related by a basic population dynamics model with apparent survival and recruitment parameters. This model had been previously applied to lek counts for greater sage-grouse *Centrocercus urophasianus* (McCaffery et al., 2016). The DM model has been found to produce acceptable estimates of abundance and detection (Kéry and Royle, 2021), but to not always being able to partitioning population growth into annual survival and recruitment (Hostetler and Chandler, 2015; Bellier et al., 2016). Hence, we developed an integrated population model (IPM), that enables one to analyze different data sets jointly and simultaneously estimate annual apparent survival, fecundity and population size using the DM model as the IPM core (Hostetler and Chandler, 2015; Kéry and Royle, 2021; Schaub and Kéry, 2022). Thus, in our IPM we integrated the DM and other available data sources (radio-tagged birds' data and counts of fledging and adults in productivity sample areas) which, although only partially aligned in space and time, allowed us to obtain improved parameter accuracy and precision (Zhao et al., 2021), and thus inferences on population-level processes. The use of the DM as core of IPM is the main difference from IPMs based on capture-recapture models, which are individual-based models which require replicate data for multiple animals that are individually identifiable (Schaub and Kéry, 2022). Lastly, in view of our results, we propose future management actions and monitoring activities.

## 2. Material and methods

### 2.1. Study area

The range of the Cantabrian capercaillie in the 1970s included the Spanish provinces of Asturias, Cantabria, León, Lugo and Palencia (Castroviejo et al., 1974). Unlike the rest of the species' range, where capercaillie live in coniferous forests, here they occur mainly in deciduous woodland, including birch (*Betula pubescens*) forest, mature beech (*Fagus sylvatica*) forest, mixed forests of beech, and sessile oaks (*Quercus petraea*,

*Q. pyrenaica*), at elevations ranging from 800 to 1800 m (Quevedo et al., 2006). This population is isolated from the nearest neighboring population in the Pyrenees in the East by more than 300 km, and was described in 2004 as restricted to an area of a 1700 km<sup>2</sup> (Storch et al., 2006).

## 2.2. Population size

### 2.2.1. Sample collection

In 2018 we carried out an intensive survey in all areas recently (2014–2018) known to be occupied to locate all occupied patches, looking for droppings, feathers and spotting birds at leks as well as in surrounding areas. We delineated those patches over a forest layer in a GIS, which resulted in a total area of 5023 ha. Then, we divided the habitat patches associated with the known leks into a total of 277 sampling units of an average of 18 ha (range 4–30 ha). In the SCR analysis (see below), we treated each sampling unit as an effective trap (Augustine et al., 2020; Mollet et al., 2015). Rangers then carried out a new survey in 2019 in all occupied areas that were previously detected in 2018. In all units, they collected capercaillie droppings below roosting trees and other commonly used places, registering the coordinates of the search path and of all collected samples using GPS devices. One or two surveys of each unit were carried out. The first survey round was conducted between 16 April and 5 May 2019, and the second between 13 May and 5 June 2019 (see Fig. S1: map of the centroids sampled, with total of samples).

### 2.2.2. DNA extraction, molecular markers and genotyping

All pre-PCR procedures for DNA extractions and amplification were conducted under DNA-free conditions and positive air pressure in dedicated rooms. Given the known difficulty of DNA extraction from capercaillie droppings (Pérez et al., 2011), we tested five DNA extraction protocols and selected the one with the best amplification results for the selected markers (Table S1). DNA was extracted from all samples using the MagMax CORE Nucleic Acid Purification kit (THERMOFISHER) in sets of 31 samples plus a negative control to monitor possible cross-contaminations. Potential PCR inhibitors were removed after DNA extraction using pre-rinsed Microcon® YM-30 centrifugal Filter Units (MILLIPORE).

Individual multilocus genotypes were determined for a set of 18 microsatellites from *T. urogallus* ( $n = 9$ ; Segelbacher et al., 2000) or related species ( $n = 6$ , Piertney and Höglund, 2001;  $n = 1$ , Piertney and Dallas, 1997;  $n = 2$ , Caizergues et al., 2001) using primers designed for low quality DNA (Pérez et al., 2011). Markers were optimized in four multiplex reactions using DNA extracted from feathers. Additionally, samples were screened for sex following Griffiths et al. (1998). All amplifications were performed using the Multiplex PCR Kit (QIAGEN) in 10  $\mu$ L final volume reactions following a pre-amplification protocol (Piggott et al., 2004). DNA quality in each sample was assessed based on the amplification of four replicas for one PCR multiplex (MP3). Samples successfully genotyped for MP3 were amplified a minimum of four times for the remnant markers. Negative controls were included throughout amplifications to monitor possible DNA cross-contamination. Marker description, multiplex sets, and PCR conditions are provided in Tables S2 & S3. PCR products were separated by size on an ABI3130xl genetic analyzer together with the GeneScan-500 LIZ size standard. Alleles were scored using GENEMAPPER 4.1 (Applied Biosystems) and checked independently by two people.

### 2.2.3. Molecular data analysis

Genotypes scored over each amplification replica were assembled for each sample in consensus genotypes following rules given in Godinho et al. (2015). Consensus genotypes with <12 microsatellites were excluded. Final genotypes were then used to assign samples to individuals and to estimate the probability of identity, i.e., the probability of identical genotypes being shared by chance between two random individuals in the population (PID) or between siblings (PIDsibs), using Gimlet 1.3.3 (Valière, 2002). To account for missing data, PID and PIDsibs were also calculated for five subsets of 12 randomly selected markers from the initial set (corresponding to the minimum number of loci genotyped in the dataset). Gimlet was used to

evaluate mean error rates of genotyping (allelic dropout and false alleles) across the 18 loci for the whole dataset. For a population genetics evaluation, individual genotypes were used to estimate nuclear diversity of the Cantabrian capercaillie based on descriptive statistics (number of alleles per locus, observed and expected heterozygosity) and to estimate departures from Hardy–Weinberg equilibrium using GenAlEx 6.5 (Peakall and Smouse, 2006). Statistical significance was adjusted using sequential Bonferroni corrections.

### 2.2.4. SCR model for population size estimation

The SCR model assumes that individual activity centers  $i = 1, 2, \dots, N$  are distributed over a region or set of points denoted the state space  $S$  (Royle et al., 2014), and individuals are exposed to sampling by some detector array within  $S$ . In our study the detector array was represented by the centroids of the 277 sampling units, with all “captures” (samples identified) assigned to the locations of those centroids (Augustine et al., 2020; Mollet et al., 2015). Only some of the samples were successfully genotyped at an individual level, and we assumed this random loss of information had no effect on the SCR analysis (Mollet et al., 2015). We assumed the population was closed over the 3-month total duration of the field work and pooled the two samples into a single, unit-specific encounter frequency for each individual  $i$  and centroid  $j$  ( $y_{ij}$ ).

The distribution of individual activity centers  $\mathbf{s}_i = (s_{i1}, s_{i2})$  in SCR models is typically described by a homogeneous, latent point process, such that  $\mathbf{s}_i \sim \text{Uniform}(S)$ . In our case  $S$  is identical to the set of all 277 sample units, since we are confident that no Cantabrian capercaillies lived anywhere else. The activity centers are latent variables to be estimated by the SCR model based on the trap-specific encounters for the  $n$  observed individuals at centroids  $j = 1, 2, \dots, J$  with locations  $\mathbf{x}_j = (x_{j1}, x_{j2})$ . Assuming that encounter frequencies are Poisson-distributed, with an encounter rate that is a decreasing function of the distance  $d$  between individual activity center  $s_i$  and centroid location  $\mathbf{x}_j$ , the encounter rate can be specified under the traditional half-normal detection function as (Royle et al., 2014):

$$\lambda_{ij}(s_i, \mathbf{x}_j) = \lambda_0 \cdot \exp\left(-\frac{d_{ij}^2}{2\sigma^2}\right)$$

where  $\lambda_0$  is the baseline detection rate (expected encounter rate when  $d_{ij} = 0$ ) and  $\sigma$  is the scale parameter of a half normal distribution—inducing a monotonous decline with distance from activity centers of individuals—that in our application of an SCR model described the movement of individuals around their activity center.

We used the scaled total sampling effort  $L$  (combined search path length for the one or two sampling occasions) in each sample unit  $j$  as a covariate for  $\lambda_0$ ,  $\beta_0$  and  $\beta_1$  are sex-specific intercepts and slopes of the log-linear regression, and  $\varepsilon$  is a random effect to account for site-level heterogeneity in the baseline detection rate:

$$\lambda_{0j} = \beta_0 + \beta_1 \times L_j + \beta_2 \times L_j^2 + \varepsilon_j$$

For each of the  $j$  traps we specified the random effect  $\varepsilon$  as a draw from a zero-mean normal distribution with a variance that was estimated from the data. This term in the model takes account of trap-specific variability that could not be assigned to known sources of detection heterogeneity.

Because sample units have variable areas, we assumed that the prior density of activity centers was in proportion to the areas of each unit. This means that our assumption of a uniform distribution of activity centers is translated into the equivalent assumption that  $s_i$  is a categorical random variable with cell probabilities given by the proportional area of each sample unit (see below). Thus, we assumed each of the activity centers  $s_i$  of the individuals of the population was associated with one of the 277 centroids of the sample units:

$$s_i \sim \text{Categorical}(\pi_1 \dots \pi_{277})$$



where the probability that  $s_i$  lies in unit  $j$ ;  $\pi_i = A_j / \sum A_j$ , where  $A_j$  is the area of each sample unit.

We used data augmentation to estimate the number of missed individuals in the sampled population (Royle et al., 2007). The likelihood for the augmented encounters  $y_{ij}$  is then modified by a partially latent binary indicator variable  $z_i$  that describes the membership of individual  $i$  to the sampled population:

$$y_{ij} | z_i \sim \text{Poisson}(\lambda_{ij} \cdot z_i)$$

Under this specification,  $Pr(z_i = 1) = 1$  for the  $n$  observed individuals, and  $z_i \sim \text{Bernoulli}(\psi)$  for all  $M$  individuals, including the augmented data. Population size is derived from the sum of indicators,  $N = \sum_1^M z_i$ .

We used model selection by Watanabe-Akaike information criterion (WAIC; Watanabe, 2013) to explore several different variations of this basic model comparing different formulations for the baseline encounter rate  $\lambda_0$ : with and without sex-related variation in the intercept and the slope on effort and in the variance parameter governing the magnitude of the trap random effects. Dey et al. (2019) reported that in SCR models WAIC selection may not be optimal. Hence, we tested as well the goodness of fit (GoF) of the models by computation of a Bayesian  $p$ -value (Royle et al., 2014, page 232) based on the posterior predictive distribution of the data (Gelman et al., 1996).

### 2.3. Change in distributional range

We scanned the distribution map of Castroviejo et al. (1974) and georeferenced and digitized it using ArcGIS 10.5. This map contained the forest fragments known to be occupied, with a subjective categorization according to the capercaillies observed. A 2-km buffer (Pollo et al., 2003) was added to those forest fragments that contained known leks, to obtain the distribution in the 1970s, using criteria and definitions of the IUCN (2001a, 2001b), which defines “area of occupancy” as the smallest area essential for the survival of a population, delineated by a circle of 2 km radius around the occupied leks. The same buffer was applied to characterize the current distribution based on the data from 2019.

### 2.4. Population trajectory: IPM for inference about long-term population dynamics

We built an integrated population model (IPM: Kéry and Royle, 2021: p. 620) that was based on a Dail and Madsen (2011) model at its core and had constant parameters over time for parsimony (Supplementary materials). Our IPM combined three different data sets via one sub-model for each (all are described in more detail below): 1) A Dail-Madsen (DM) likelihood for the repeated counts in a robust-design format (Dail and Madsen, 2011; Hostetler and Chandler, 2015), 2) a multistate likelihood for the capture-recapture data (MS-CR), and 3) a reproduction (RM) model from counts of fledgings and adults (Rajala, 1974) in the sampled study areas. Both annual survival and recruitment parameters appear in both the DM and the MS-CR ( $\phi$ ) and in those of DM and RM ( $\gamma$ ) respectively. Thus, these parameters form the links between the three sub-models. It is this linkage that represents the integration of the information in the three datasets and specifies the joint likelihood as a product of the three separate likelihoods under the usual independence assumption. We used in the IPM a moderately informative prior for  $\phi$  that gives less mass to very small and very large values of annual survival (Schaub and Kéry, 2022) which are a priori extremely unlikely for this large species. To test its effect, we compared priors used and posterior distributions and point estimate of  $\phi$  and  $\gamma$ , using both models with this informative prior and for comparison with a less informative prior as an alternative.

1) The DM model is a hierarchical state-space model for count-based population dynamics that accommodates imperfect detection in the observation model and includes three conditionally related processes corresponding to: (1) initial abundance; (2) abundance at time  $t$  (for  $t$

$> 1$ ) conditional on abundance at  $t - 1$  and on parameters of apparent annual survival ( $\phi$ ) and recruitment ( $\gamma$ ); and (3) the detection process (Hostetler and Chandler, 2015). In our DM we use count data from 1978 to 2019, i.e. over 42 years. As the monitoring effort was not uniform across the years, the data array had a high number of missing values (81% of missing values per site  $\times$  year). To avoid having to update those missing values in the Bayesian implementation, we rewrote the DM BUGS model (Kéry and Royle, 2016, page 105) to use the data in “long” format (Kéry and Royle, 2016, page 264), which supplies only the non-missing counts as data. Due to the large amount of missing data only the Julian date covariate and a random site effect could be tested on the probability of detection.

2) MS-CR sub-model: We used the data from 33 radio-telemetry tagged individuals (1997–2020) to make inferences about the apparent annual survival. We distinguished 4 true states: 1) alive-juvenile; 2) alive-adult; 3) recently dead and recovered and 4) recently dead, but not recovered, or dead (absorbing) (Supplementary materials). The matrix  $\mathbf{z}$  with element  $z_{i,t}$  indicates the true state of individual  $i$  at time  $t$ . The state-transition matrix ( $\mathbf{\Omega}$ ) has four dimensions: the first and second dimension of  $\mathbf{\Omega}$  denote the states of departure and of arrival, respectively, the third dimension the individual ( $i$ ), and the fourth-dimension time ( $t$ ). Element  $\omega_{n,m,i,t}$  of  $\mathbf{\Omega}$  is the probability that individual  $i$ , which is in state  $n$  at time  $t$ , is in state  $m$  at time  $t + 1$ . Similarly, the observation matrix ( $\mathbf{\Theta}$ ) has four dimensions, where the second is the observed state, and its elements  $\varphi_{n,m,i,t}$  are the probability that individual  $i$ , which is in state  $n$  at time  $t$ , is observed in state  $m$  at time  $t$ .

The development of the state membership over time is:

$$z_{i,t} | z_{i,t+1} \sim \text{Categorical}(\mathbf{\Omega}_{z_{i,t},1,\dots,A,i,t})$$

while the observation equation links the true state with the observed state:

$$y_{i,t} | z_{i,t} \sim \text{Categorical}(\mathbf{\Theta}_{z_{i,t},1,\dots,A,i,t})$$

We made the usual multistate model assumptions that individuals and states are recorded without error and that no tags are lost (Kéry and Schaub, 2012).

3) RM sub-model: We estimated per-capita recruitment from the observed reproduction rate during July–October using bivariate counts (i.e., juveniles and adults) in sampled areas from 1997 to 2010 and 2018–2020 (Benito, 2019; García-Fernández and Benito, 2016; unpublished data from authors).

An important caveat regarding an IPM is that if one of the data types in some of the sub-models is “biased” (in the sense of being atypical or not representative for the population under study), then, through sampling covariance, this bias can propagate to estimates that would not have been affected if the different data types had been analyzed separately (Péron et al., 2012). The absence of such bias in an IPM has also been called the “common-demography assumption” by Schaub and Kéry (2022). In our case study we use a DM as IPM core, and this model is known to struggle sometimes to separate recruitment and annual survival with count data alone (Bellier et al., 2016; Hostetler and Chandler, 2015; Kéry and Royle, 2021, page 124; Zipkin et al., 2014). We expected our data from the multistate capture-recapture sub-model -which uses marked animals- could a priori permit better estimates of survivals and thus that it would improve the IPM estimates. Nevertheless, to test the influence of the different sub-models, we compared the IPM estimates with those from the MS-CR model alone, and we compared the output of the Dail-Madsen model alone with that of the IPM (with one and two sub-models) and the overlap of posterior probability density of the parameters from each. With a larger overlap of the component data, we can be more confident they are describing the same underlying demographic patterns (Schaub and Kéry, 2022). We also measured the reduction in coefficient on variation (ratio of the standard deviation to the mean) in those combinations (Péron et al., 2012). In addition, we inspected the correlation matrix of the estimated

**Table 1**

Model selection in spatial capture-recapture (SCR) analysis using the Watanabe-Akaike information criterion (WAIC).  $\sigma(\text{sex})$  denotes the sex-specific scale parameter for the half-normal detection function, related to movement of animals;  $\lambda_0$  is the baseline detection rate, with effects of sex, linear and quadratic from effort; and a random trap effect (RandEff) with either constant precision (RandEff[trap]) or with sex-specific precision (RandEff[trap[sex]]).

Model	WAIC	$\Delta$ WAIC
$\sigma(\text{sex}) \lambda_0(\text{sex} + \text{effort}[\text{sex}] + \text{effort}[\text{sex}]^2 + \text{RandEff}[\text{trap}[\text{sex}]])$	1639.25	0.00
$\sigma(\text{sex}) \lambda_0(\text{sex} + \text{effort}[\text{sex}] + \text{effort}[\text{sex}]^2 + \text{RandEff}[\text{trap}])$	1655.86	16.61
$\sigma(\text{sex}) \lambda_0(\text{sex} + \text{effort}[\text{sex}] + \text{effort}[\text{sex}]^2)$	1836.48	197.23
$\sigma(\text{sex}) \lambda_0(\text{sex} + \text{effort}[\text{sex}])$	1867.26	228.01

parameters in SCR and IPM models to study the apparent compensatory heterogeneity (Broekhuis et al., 2021).

**2.5. Model implementation**

All SCR and IPM models were fitted using Bayesian inference with software NIMBLE (version 0.11.1; NIMBLE Development Team, 2019) in R (R Core Team, 2020). In SCR models we ran three chains of 25,000 iterations and an initial 5000 as a burn-in. For IPM models we ran 500,000 iterations with an initial 200,000 iterations as a burn-in, and thinned the remainder by 10. In IPM we used the WAIC to rank candidate model fit using MCMC (three chains of 10,000 iterations, discarding the first 5000 as a burn-in). In SCR models we used selection by WAIC and computed Bayesian  $p$ -values with three chains of 5000 iterations and 1000 as burn-in each case. Additionally, we used the GoF test suggested by Meredith (2020). We assessed model convergence by examining trace plots visually and using estimates of effective sample size and split-chain  $\hat{R}$ , which can be used to better diagnose convergence failure of MCMC chains (Vehtari et al., 2020). We report the posterior mean for point estimates and 95% percentiles for Bayesian credible intervals (BCI).

**3. Results**

**3.1. Population size**

**3.1.1. Sampling and individual identification**

Linear sampling effort totaled 228.5 km (101.4 m/ha) in Asturias region and 342.4 km (123.5 m/ha) in Castilla y León region, resulting in an

average of 117 (SD: 69.2) m/ha. We collected 771 samples; 314 (0.14 samples/ha) in Asturias and 457 (0.16 samples/ha) in Castilla y León.

We successfully genotyped 308 samples corresponding to 120 (80 males, 39 females and 1 unknown) individuals. Average missing data per genotype was 6.6% (2.4 out of 18 markers). The whole dataset achieved a probability of identity  $\text{PID} = 1.40 \times 10^{-9}$  and a  $\text{PIDsibs} = 7.13 \times 10^{-5}$ , with the expected number of individuals and siblings sharing an identical genotype by chance ( $\text{PID} \times \text{sample size}$ ) of  $1.68 \times 10^{-7}$  and  $8.56 \times 10^{-3}$ , respectively. These values strongly support that the identical genotypes accurately identify the same individual. Likewise, the five subsets of 12 randomly selected markers also showed very low values for PID and PIDsibs (Table S5), consistently validating the use of genotypes up to a minimum of 12 markers. We “recaptured” (i.e., collected and genotyped more than one sample from the same individual) 62 individuals, corresponding to 42 males and 20 females, captured on average 4.6 (range = 1–13) and 4.2 (range = 1–11) times, respectively. Of those recaptured we have 26 males (30%) and 14 females (42%) with spatial recaptures. Thus, we found 80 individuals in one “trap” (sample units); 30 in two traps; 9 in three traps, and 1 in four traps.

Cantabrian capercaillies exhibited low to medium genetic diversity, with a mean observed number of alleles per locus of  $3.5 \pm 0.3$ , and mean observed and expected heterozygosity of  $0.47 \pm 0.03$  and  $0.53 \pm 0.03$ , respectively (Table S4). Two loci showed significant deviations from Hardy-Weinberg expectations ( $p < 0.001$ ; Table S4) and were not considered for genetic diversity evaluation. Average error rates were high but still within expected values for noninvasive samples. Estimated allelic dropout rate across loci was  $\text{ADO} = 0.26$  ( $0 < \text{ADO} < 0.41$ ), and false alleles were  $\text{FA} = 0.01$  ( $0 < \text{FA} < 0.14$ ; see Table S5 for individual values per marker).

**3.1.2. SCR: model selection and population size estimate**

Model selection using WAIC among two variants in the SCR model selected (Table 1) a model with a random effect for baseline detection rate allowing different values for each sampling unit, which had higher predictive accuracy than a model without the random effect. The goodness of fit (GoF) for the model without a random effect (Figs. S2 and S3) was poor. GoF for the selected model including a random effect (Figs. S4 and S5) indicated a better model fit, but still showed some lack of fit in the first component. Therefore, WAIC model selection and GoF assessment were consistent in these analyses.

The best model resulted in an estimated population size estimate (Table 2) of 191 (165–222) individuals (Table 2; Fig. 1); 60 (48–78)

**Table 2**

Marginal posterior summaries for the WAIC-best spatial capture-recapture (SCR) model (see Table 1) for the Cantabrian capercaillie population in 2019. Posterior means are used as point estimates, and 95% Bayesian credible interval (BCI) as interval upper and lower bounds.  $N$  is the population size (total, females and males); parameters  $\alpha_0$ ,  $\alpha_1$  and  $\alpha_2$  are, respectively, the intercept and the linear and quadratic effects of effort, stratified by sex, in the baseline detection rate ( $\lambda_0$ ), while  $\tau$  denotes the sex-specific precision of the trap random effect.  $\psi$  is the data augmentation parameter, and  $\sigma$  is the sex-specific half-normal scale parameter (in meters). Bulk\_ ESS and Tail\_ ESS are crude measures of effective sample size for bulk and tail quantities, respectively (an ESS > 100 per chain is considered good), and  $\hat{R}$  is the potential scale reduction factor on rank normalized split chains (at convergence,  $\hat{R} \leq 1.05$ ).

	Mean	SD	BCI			$\hat{R}$	Bulk_ ESS	Tail_ ESS
			2.50%	50%	97.50%			
$N[\text{total}]$	190.61	14.44	165.00	190.00	222.00	1.00	2341	7391
$N[\text{females}]$	60.16	7.66	48.00	59.00	78.00	1.00	2980	8484
$N[\text{males}]$	130.45	12.23	109.00	130.00	157.00	1.00	2231	6880
$\text{Sex-ratio}$	0.684	0.033	0.614	0.686	0.744	1.00	2651	7991
$\alpha_0[\text{f}]$	-2.126	0.338	-2.836	-2.107	-1.515	1.00	568	1394
$\alpha_0[\text{m}]$	-2.292	0.281	-2.840	-2.287	-1.750	1.01	532	1129
$\alpha_1[\text{f}]$	1.330	0.317	0.759	1.310	1.998	1.00	971	2134
$\alpha_1[\text{m}]$	1.443	0.303	0.863	1.438	2.047	1.00	465	1040
$\alpha_2[\text{f}]$	-0.469	0.155	-0.811	-0.459	-0.199	1.00	1142	2396
$\alpha_2[\text{m}]$	-0.419	0.126	-0.670	-0.417	-0.181	1.01	447	829
$\tau[\text{f}]$	0.765	0.349	0.345	0.690	1.594	1.00	3834	8795
$\tau[\text{m}]$	0.332	0.065	0.253	0.318	0.493	1.00	2978	6976
$\psi$	0.308	0.030	0.254	0.307	0.370	1.00	375	723
$\sigma[\text{f}]$	269.2	55.8	181.6	262.2	397.1	1.00	838	1485
$\sigma[\text{m}]$	107.6	14.0	82.9	106.6	137.6	1.00	3754	6424

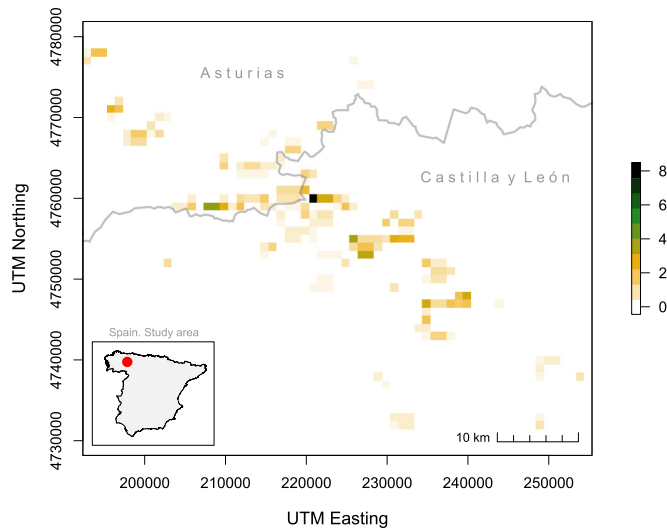


**Fig. 1.** Posterior means of abundance of the Cantabrian capercaillie in the surveyed sampling units (summarized by the estimated number of activity centers per 1 Km<sup>2</sup> grid cell).

females and 130 (109–157) males. This suggested that only 62% and 65% of the males and females, respectively, were detected at all, in spite of our intensive survey. Sex ratio (males/population size) was estimated at 0.68 (0.61–0.74). Baseline detection rate depended on sex and sampling effort (Table 1). The half normal scale parameter ( $\sigma$ ) was estimated at 269 (181–397) meters for females and at 108 (83–138) meters for males (Table 1). We did not find high correlations between posterior parameters that could indicated apparent compensatory heterogeneity (Fig. S6).

**3.2. Change in distributional range**

The original distribution area based on information from Castroviejo et al. (1974) was estimated at 5281 km<sup>2</sup>. Currently, the range was

estimated at only 923 km<sup>2</sup>, representing a reduction of 83%. The easternmost part of the original population has completely disappeared, while the remaining population occupies a rather narrow strip in the western area (Fig. 1 and Graphical abstract).

**3.3. Population trajectory inferred by the IPM**

The WAIC-best IPM suggested a very strong population decline on the Southern slope of the Cantabrian range from 1110 (95% BCI 1000–1233) birds in 1978 to only 85 (67–107) in 2019 (Fig. 2 and Table S6), amounting to a decline of more than 90% in just over 40 years. Julian date and a random site effect were selected in detection probability (Table 3).

Apparent annual survival ( $\phi$ ) under the WAIC top IPM was estimated at 0.707 (0.677–0.735), and per-capita recruitment ( $\gamma$ ) at 0.233 (0.207–0.262). Using the MS-CR model alone, the average (over sexes) apparent annual survival was very close to the estimate under the IPM;  $\phi = 0.702$  (0.602–0.792), with male annual survival estimated at  $\phi_M = 0.736$  (0.607–0.849) and female annual survival at  $\phi_F = 0.651$  (0.499–0.788).

The population trajectory from the DM model alone was very close to that inferred by the full IPM, but we found slight differences in annual survival (0.788 vs 0.702) and in per-capita recruitment (0.154 vs 0.233) between DM and IPM, respectively. The use of an informative prior on  $\phi$  had a limited effect on posterior estimates (Fig. S7 and Table S7). Changes induced in the estimated population size in DM and IPM models by changes in annual survival and per-capita recruitment were minimal (Table S8). The posterior densities of each sub-model largely overlapped for both main parameters (Fig. S8), and hence we don't expect a disproportionate influence of either in the IPM. Results (Table S8) using DM; DM + MS capture-recapture, and the full IPM (DM + MS capture-recapture + Reproduction) indicated that using all of the available data in our IPM reduced the coefficient of variation in all main parameters of interest: annual survival ( $\phi$ : 0.026; 0.023 and 0.021) and per-capita recruitment ( $\gamma$ : 0.116; 0.084 and 0.060) without inducing any significative bias on initial population estimate (0.053; 0.058 and 0.054, respectively).

We did find a high negative correlation between the estimates of the per-capita recruitment ( $\gamma$ ) and apparent annual survival ( $\phi$ ) (Figs. S9 and S10). This is not surprising and is simply an expression of the known challenge to parse out the population growth rate into these two components (Bellier et al., 2016). Goodness-of-fit tests for the DM sub-model from IPM indicated an adequate model fit ( $p = 0.59$ ; Fig. S11).

**4. Discussion**

We used state of the art field and analytical techniques to provide a comprehensive assessment of the current status and long-term trends of the Cantabrian capercaillie in its entire range and in the Southern slope of it

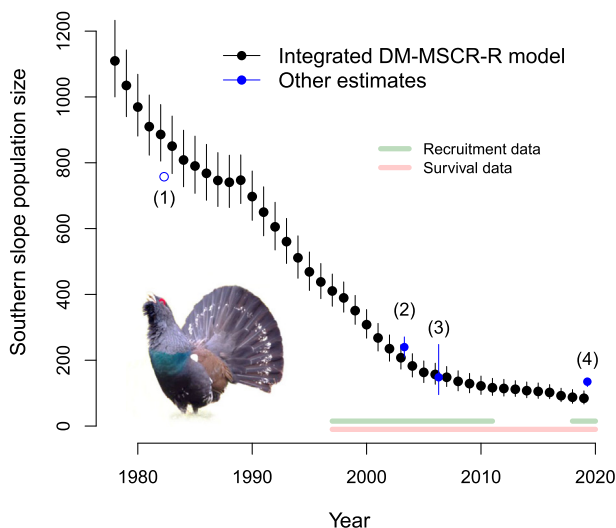


**Fig. 2.** Estimated trajectory of the Cantabrian capercaillie population on the Southern slope (in black) using an integrated Dail Madsen-Multistate Capture Recapture-Recruitment model (posterior means with 95% BCIs) and comparison (in blue) with other estimates: (1) inferred: blue circle (results corrected using the average detection probability  $p = 0.77$  from the IPM model, and considering 50% population in Southern slope) from del Campo and García-Gaona (1983); and in solid blue: (2) Pollo et al. (2005); (3) Vázquez et al. (2013), assuming a 50% in the Southern slope, and (4) this study.

**Table 3**

Model selection in the integrated population model with at its core the Dail Madsen-Multistate Capture Recapture-Recruitment. We compared *Initial Abundance* ( $\lambda$ ) using Negative Binomial (NB) or a Poisson distribution; *Detection probability* ( $p$ ) with Julian date (and its quadratic effect), and *Dynamics* (per-capita recruitment ( $\gamma$ ) and apparent annual survival ( $\phi$ ) with autoregressive (with and without immigration) models.

Model	WAIC	$\Delta$ WAIC
<b>Initial abundance</b>		
Poisson[A(.)]Autoregres[Γ(.)Φ(.)]p(.)	3401.08	0.00
NB[A(.)]Autoregres[Γ(.)Φ(.)]p(.)	3417.11	16.03
<b>Detection probability</b>		
Poisson[A(.)]Autoregres[Γ(.)Φ(.)]p(JD + RE)	3249.71	0.00
Poisson[A(.)]Autoregres[Γ(.)Φ(.)]p(JD)	3289.01	39.30
Poisson[A(.)]Autoregres[Γ(.)Φ(.)]p(.)	3401.08	151.37
<b>Dynamics</b>		
Poisson[A(.)]Autoregres + Imm[Γ(.)Φ(.)]p(JD + RE)	3221.33	0.00
Poisson[A(.)]Autoregres[Γ(.)Φ(.)]p(JD + RE)	3249.71	28.39



respectively. Using the SCR model, we estimate that currently only 191 (165–222) capercaillie individuals remain in the whole Cantabrian Mountains. Our analyses also show a male bias in the sex ratio, although this may be partly related to a methodological issue related to our sampling at leks. If nesting areas coincide with leks, then the detectability of females is likely to be similar to that of males. However, if nesting areas do not overlap with leks, females will be less detectable, and their detection will depend on the duration and temporal pattern of their visitation scheme at the leks. This will result in detection heterogeneity, which then might lead to an underestimation of the female part of the population. Despite this possible underestimation of number of females, there is likely a substantial genuine bias in the sex ratio, as has been described in this and other populations (Bañuelos et al., 2019; Mollet et al., 2015; Santorek et al., 2021) and which will have a demographic impact and should be considered in population management. It is also possible that we missed a small number of males that did not attend leks. However, we believe that the possible number of such cases was minimal and thus that our current population size assessment was accurate.

Focusing on the decline of the capercaillie across the entire range of the Cantabrian Mountains, population loss has been spatially very non-uniform, moving from E to W and just so slightly from N to S, without any ready explanation for that pattern. In global figures, the capercaillie currently occupies only 17% of its range in the 1970s. Nevertheless, the presence of isolated individuals in the eastern parts of the former range cannot be entirely ruled out. Currently, the most recent observation dates from at 11 October 2021 (F. Ibáñez, pers. comm.) and was made in a firewood extraction area, which after forest thinning had grown a dense cover of bilberry *Vaccinium myrtillus*.

The dynamics of the population on the Cantabrian southern slope show an annual loss of population size of around 5.9% on average. In our IPM we assumed the vital rates are density-independent and did not change over time. The latter assumption may be unrealistic over long periods of time, and in this sense, our estimate should be considered as a simplification of the actual process that has been taking place. Despite this caveat, we are confident that the overall trajectory of the population is adequately described by the model presented here. DM models, which form the core of our IPM, have previously been found to produce good estimates of abundance and detection from counts of unmarked individuals (Bellier et al., 2016; Hostetler and Chandler, 2015; Kéry and Royle, 2021, page 31–47; Kidwai et al., 2019) even with fairly sparse data (McCaffery et al., 2016). There are no reliable references for comparison of this inference from our IPM, since prior to the 1970s, information about Cantabrian capercaillie population sizes was fragmented and scarce. Nevertheless, Fig. 2 shows that population size estimates under our IPM are remarkably consistent with independent data from the archives of the Spanish Government (Servicio Nacional de Pesca Fluvial y Caza in Castroviejo et al., 1974), and only slightly higher (Fig. 2) than what was reported by del Campo and García-Gaona (1983).

Regarding the accuracy of estimates of demographic parameters, possible compensatory biases in recruitment and survival estimates have been highlighted in DM models (Hostetler and Chandler, 2015). Kéry and Royle (2021, page 624) partially resolved such biases by adding in other data sources and developing an integrated Dail-Madsen capture-recapture-recruitment model. However, even in those models, annual survival appeared to be biased when a comparison was made between the estimates under the integrated model and the CR model alone. In contrast, in our IPM, the apparent annual survival resulting from the integrated model is very close to that produced by the MS-CR model alone (0.707 vs 0.702). Therefore, in view of the IPM result and its comparison with DM model and combinations of sub-models, we are confident that the IPM vital parameters estimate would be adequate. We are using more informative data than just the simple counts on which the survival-recruitment partitioning is based in a DM model alone, which can sometimes be biased towards overestimation of survival (Kéry and Royle, 2021). The correlation we found between the estimates of recruitment rate and apparent annual survival in the IPM (Fig. S11) agrees with what was pointed out by Bellier et al.

(2016) and Kéry and Royle (2021): i.e., that there was a trade-off between apparent survival and recruitment in the Dail-Madsen model. Comparison of the estimates of apparent annual survival among different capercaillie populations (presented in Table 4) reveal similar or only slightly higher values than ours for the Cantabrian capercaillie. However, it should be noted that in our study the annual survival estimates include both the juvenile and the adult part of the population. Additionally, per-capita recruitment for the Cantabrian capercaillie is lower than that reported by other authors (Table 4).

Our results suggest an extremely dire situation for the survival of the Cantabrian capercaillie over even a medium term. Although apparent annual survival is similar to that estimated in other populations, it is typically the most important demographic driver for a long-lived species (Bal et al., 2021) and should be studied to be incorporated accurately in future management actions. Recruitment also seems to be insufficient to maintain the population. A similar scenario was described by Moss et al. (2000) and by Augustine et al. (2020) in Scotland and in Switzerland, respectively (Table 4). Management efforts to improve recruitment have been proposed in Spain to preserve the capercaillie population in the Pyrenees (Fernández-Olalla et al., 2012; Moreno-Opo et al., 2015). Although our study did not allow us to identify covariates affecting recruitment, some authors have suggested several factors linked to forest structure (Kortmann et al., 2018), climate change (Moss et al., 2001), predation (Jahren et al., 2016) and ground cover of bilberry (Baines et al., 1994). Bilberry supports abundant invertebrates, which together with bilberry leaves and berries, have been described as constituting a large part of the chick diet (Kastdalen and Wegge, 1985; Picozzi et al., 1996). Baines et al. (2004) estimate that bilberry should ideally cover 15–20% of the ground, but we noted that the productivity of bilberry is also related to grazing and ungulate browsing pressure.

The protection of the capercaillie in Spain during the last decades has been mainly based on passive conservation. The overall development of the vegetation in the Cantabrian mountain range has been towards a dense forest structure, with only sparse and spatially limited ground cover. In this context, even accepting the fact that may be possible that climate change could be a main driver in the decline, we emphasize that there is still room to develop a more active management, where forest management for capercaillie conservation should be implemented, considering as well the management of wild and domestic ungulates. Studying the chick diet in the Cantabrian Mountains (e.g. using DNA-metabarcoding), to improve the productivity of the target species (e.g. bilberry) should be a priority. Predation management had also been suggested as a tool to improve survival and recruitment of the species (Jahren et al., 2016; Kämmerle and Storch, 2019; Moreno-Opo et al., 2015; Summers et al., 2009) and it is currently implemented in the Cantabrian Mountains in an experimental manner. This measure should include other related activities, like the removal of carcasses of hunted ungulates to avoid increasing food resources of mesocarnivores (Tobajas et al., 2021). Future management responses should also consider the genetic viability of this population, and might implement an ex-situ conservation program with a strong genetic basis and subsequent reintroduction program of an adequate number of individuals. This is planned in the Strategy for Conserving the Cantabrian Capercaillie

**Table 4**

Previous estimates of the two demographic rates, apparent annual survival and per-capita recruitment rate for capercaillies in Western Europe as published in the literature.

References	Sex	Survival	Recruitment rate	Study area
(Leclercq, 1987)	Female	0.82	–	Jura Mountains (France)
(Moss et al., 2000)		0.72 (0.60–0.81)	0.280	Scotland
(Bañuelos et al., 2019)	Male	0.85–0.90	–	Cantabrian Mountains
	Female	0.49–0.59	–	
(Augustine et al., 2020)	Male	0.76 (0.71–0.81)	0.127	Switzerland
	Female	0.71 (0.63–0.77)	0.115	

(CNPN, 2004) and is currently in the early implementation phase. It is also a priority to assess the impact of potential drivers of recruitment and survival, using management activities in response to identified issues. The use of Bayesian networks and an associated monitoring program is recommended for the implementation of an iterative decision-making, evaluating results and adjusting actions (Holling, 1978) both for current and potential future management actions.

### CRedit authorship contribution statement

**José Jiménez:** Conceptualization, Data curation, Formal analysis, Investigation, Methodology, Resources, Software, Supervision, Validation, Visualization and Writing – original draft. **Raquel Godinho:** Conceptualization, Data curation, Formal analysis, Investigation, Resources, Methodology, Software, Writing - review & editing. **Daniel Pinto:** Data Curation, Investigation, Project administration. **Susana Lopes and Diana Castro:** Formal analysis, Resources. **David Cubero and M. Angeles Osorio:** Funding acquisition, Investigation, Project administration. **Josep Piqué:** Investigation, Writing - review & editing. **Rubén Moreno-Opo:** Conceptualization, Funding acquisition, Project administration, Writing - review & editing. **Pablo Quirós:** Funding acquisition, Investigation, Project administration. **David Nuevo-Galán:** Funding acquisition, Investigation, Project administration. **Orencio Hernández-Palacios:** Funding acquisition, Investigation, Project administration. **Marc Kéry:** Methodology, Software, Writing - review & editing.

### Research funders information

Ministerio para la Transición Ecológica y el Reto Demográfico (18MNES002 and 19MNES001); Junta de Castilla y León (EN-16/19); Gobierno del Principado de Asturias (SCP025/2019).

### Declaration of competing interest

The authors declare that they have no known competing financial interests or personal relationships that could have appeared to influence the work reported in this paper.

### Acknowledgements

We are indebted to the forest rangers of Principado de Asturias and Castilla y León, as well as Fundación Patrimonio Natural de la Junta de Castilla y León, who collected the samples, and staff of the Ministerio para la Transición Ecológica (L. M. González, F. García) and Tragsatec (M. Pina, A. Leite, A. García, J. L. Álvarez and M. Abascal). Eva López (Principado de Asturias) contributed to the organization of sample collection and data curation for Asturias. The Central Veterinary Laboratory (Algete, Ministry of Agriculture) performed the preliminary analyses on the 2018 samples. Genetic analysis from 2019 data was done in CIBIO-InBIO (Portugal). We thank the Junta de Castilla y León for providing us the capercaillie count data 1978-2019 and J. L. Benito for his field data contribution. Dr. Mario Quevedo (University of Oviedo) kindly provided us with hard-to-find capercaillie references. F. Ibáñez (EBD-CSIC) providing us two citations of capercaillie in the eastern part of the range in 2021.

### Appendix A. Supplementary data

Supplementary data to this article can be found online at <https://doi.org/10.1016/j.scitotenv.2022.153523>.

### References

Augustine, B.C., Kéry, M., Olano Marin, J., Mollet, P., Pasinelli, G., Sutherland, C.S., 2020. Sex-specific population dynamics and demography of capercaillie (*Tetrao urogallus* L.) in a patchy environment. *Popul. Ecol.* 62, 80–90. <https://doi.org/10.1002/1438-390X.12031>.

- Baines, D., Sage, R.B., Baines, M.M., 1994. The implications of Red Deer grazing to ground vegetation and invertebrate communities of scottish native pinewoods. *J. Appl. Ecol.* 31, 776. <https://doi.org/10.2307/2404167>.
- Baines, D., Moss, R., Dugan, D., 2004. Capercaillie breeding success in relation to forest habitat and predator abundance. *J. Appl. Ecol.* 41, 59–71. <https://doi.org/10.1111/j.1365-2664.2004.00875.x>.
- Bal, G., Bacon, L., Ménoni, E., Calenge, C., Millon, A., Besnard, A., 2021. Modélisation de la dynamique du grand tétras des Pyrénées françaises pour sa gestion adaptative. <https://doi.org/10.13140/RG.2.2.16328.65285>.
- Bañuelos, M.J., Blanco-Fontao, B., Fameli, A., Fernández-Gil, A., Mirol, P., Morán-Luis, M., Rodríguez-Muñoz, R., Quevedo, M., 2019. Population dynamics of an endangered forest bird using mark-recapture models based on DNA-tagging. *Conserv. Genet.* 20, 1251–1263. <https://doi.org/10.1007/s10592-019-01208-x>.
- Bellier, E., Kéry, M., Schaub, M., 2016. Simulation-based assessment of dynamic N-mixture models in the presence of density dependence and environmental stochasticity. *Methods Ecol. Evol.* 7, 1029–1040. <https://doi.org/10.1111/2041-210X.12572>.
- Benito, J.L., 2019. Censo de productividad y radiomarcaje de urogallo cantábrico *Tetrao urogallus cantabricus* en el Principado de Asturias. 2019. Año.
- BirdLife International, 2021. Species factsheet: Tetrao urogallus [WWW Document]. IUCN Red List birds. <http://www.birdlife.org>
- Borchers, D.L., Efford, M.G., 2008. Spatially explicit maximum likelihood methods for capture-recapture studies. *Biometrics* 64, 377–385. <https://doi.org/10.1111/j.1541-0420.2007.00927.x>.
- Broekhuis, F., Elliot, N.B., Keiwua, K., Koinet, K., Macdonald, D.W., Mogensen, N., Thuo, D., Gopalaswamy, A.M., 2021. Resource pulses influence the spatio-temporal dynamics of a large carnivore population. *Ecography (Cop.)* 44, 358–369. <https://doi.org/10.1111/ecog.05154>.
- Caizergues, A., Dubois, S., Loiseau, A., Mondor, G., Rasplus, J.-Y., 2001. Isolation and characterization of microsatellite loci in black grouse (*Tetrao tetrix*). *Mol. Ecol. Notes* 1, 36–38. <https://doi.org/10.1046/j.1471-8278.2000.00015.x>.
- Castroviejo, J., Delibes, M., García-Dory, M.A., Junco, E., 1974. Censo de urogallos cantábricos (*Tetrao urogallus cantabricus*). *Asturmaturo* 2, 53–74.
- CNPN, 2004. Estrategia Para la conservación del urogallo Cantábrico en España. Ministerio de Medio Ambiente, Madrid, Spain.
- Dail, D., Madsen, L., 2011. Models for estimating abundance from repeated counts of an open metapopulation. *Biometrics* 67, 577–587. <https://doi.org/10.1111/j.1541-0420.2010.01465.x>.
- de Juana, E., Kirwan, G.M., 2020. Western capercaillie (*Tetrao urogallus*). In: del Hoyo, J., Elliott, A., Sargatal, J., Christie, D., de Juana, E. (Eds.), *Birds of the World*. Cornell Lab of Ornithology, Ithaca, NY, USA <https://doi.org/10.2173/bow.wescap1.01>.
- del Campo, J.C., García-Gaona, J.F., 1983. Censo de urogallos *Tetrao urogallus* en la Cordillera Cantábrica. *Nat. Hisp.* 25.
- Dey, S., Delampady, M., Gopalaswamy, A.M., 2019. Bayesian model selection for spatial capture-recapture models. *Ecol. Evol.* 9, 11569–11583. <https://doi.org/10.1002/eec3.5551>.
- Duriez, O., Sachet, J.M., Ménoni, E., Pidancier, N., Miquel, C., Taberlet, P., 2007. Phylogeography of the capercaillie in Eurasia: what is the conservation status in the Pyrenees and Cantabrian mountains? *Conserv. Genet.* 8, 513–526. <https://doi.org/10.1007/s10592-006-9165-2>.
- Efford, M.G., Dawson, D.K., Robbins, C.S., 2004. DENSITY: software for analysing capture-recapture data from passive detector arrays. *Anim. Biodivers. Conserv.* 27, 217–228.
- Fernández-Olalla, M., Martínez-Abraín, A., Canut, J., García-Ferré, D., Afonso, I., González, L.M., 2012. Assessing different management scenarios to reverse the declining trend of a relict capercaillie population: a modelling approach within an adaptive management framework. *Biol. Conserv.* 148, 79–87. <https://doi.org/10.1016/j.biocon.2012.01.047>.
- García-Fernández, J., Benito, J.L., 2016. Seguimiento de ejemplares de urogallo cantábrico radiomarcados en el Alto Sil (León) y Degaña (Asturias) Período octubre 2013-noviembre 2016.
- Gelman, A., Meng, X.L., Stern, H., 1996. Posterior predictive assessment of model fitness via realized discrepancies. *Stat. Sin.* 6, 733–807.
- Godinho, R., López-Bao, J.V., Castro, D., Llaneza, L., Lopes, S., Silva, P., Ferrand, N., 2015. Real-time assessment of hybridization between wolves and dogs: combining noninvasive samples with ancestry informative markers. *Mol. Ecol. Resour.* 15, 317–328. <https://doi.org/10.1111/1755-0998.12313>.
- Griffiths, R., Double, M.C., Orr, K., Dawson, R.J.G., 1998. A DNA test to sex most birds. *Mol. Ecol.* 7, 1071–1075. <https://doi.org/10.1046/j.1365-294x.1998.00389.x>.
- Holling, C.S., 1978. *Adaptive Environmental Assessment and Management*. John Wiley & Sons.
- Hostetler, J.A., Chandler, R.B., 2015. Improved state-space models for inference about spatial and temporal variation in abundance from count data. *Ecology* 96, 1713–1723. <https://doi.org/10.1890/14-1487.1>.
- Hostetter, N.J., Gardner, B., Sillett, T.S., Pollock, K.H., Simons, T.R., 2019. An integrated model decomposing the components of detection probability and abundance in unmarked populations. *Ecosphere* 10, e02586. <https://doi.org/10.1002/ecs2.2586>.
- IUCN, 2001. IUCN Red List Categories: Version 3.1. Prepared by the IUCN/SSC. IUCN, Gland, Switzerland and Cambridge, UK 23 pp.
- IUCN, 2001b. Guidelines for assessing taxa with widely distributed or multiple populations against criterion a. Prepared by the IUCN/SSC/SPS, IUCN, Gland, Switzerland and Cambridge, UK, p. 10.
- Jahren, T., Storaas, T., Willebrand, T., Fossland Moa, P., Hagen, B.R., 2016. Declining reproductive output in capercaillie and black grouse-16 countries and 80 years. *Anim. Biol.* 66, 363–400. <https://doi.org/10.1163/15707563-00002514>.
- Kammerle, J.-L., Storch, I., 2019. Predation, predator control and grouse populations: a review. *Wildlife Biol.* 2019, 1–12. <https://doi.org/10.2981/wlb.00464>.
- Karanth, K.U., Nichols, J.D., 1998. Estimation of Tiger densities in India using photographic captures and recaptures. *Ecology* 79, 2852–2862. <https://doi.org/10.2307/176521>.



- Kastdalen, L., Wegge, P., 1985. Animal food in capercaillie and black grouse chicks in south-East Norway. *International Grouse Symposium*, pp. 498–508.
- Kellner, K.F., Swihart, R.K., 2014. Accounting for imperfect detection in ecology: a quantitative review. *PLoS One* 9. <https://doi.org/10.1371/journal.pone.0111436>.
- Kéry, M., Royle, J.A., 2016. *Applied hierarchical modeling in ecology analysis of distribution, abundance and species richness in R and BUGS. Prelude and static Models*, 1st ed. Academic Press/Elsevier.
- Kéry, M., Royle, J.A., 2021. *Applied hierarchical modeling in ecology. Analysis of distribution, abundance and species richness in R and BUGS. Dynamic and Advanced Models*. 2. <https://doi.org/10.1016/c2013-0-19160-x>.
- Kéry, M., Schaub, M., 2012. *Bayesian population analysis using WinBUGS. Academic Press/Elsevier. A hierarchical perspective* <https://doi.org/10.1016/B978-0-12-387020-9.00014-6>.
- Kidwai, Z., Jiménez, J., Louw, C.J., Nel, H.P., Marshal, J.P., 2019. Using N-mixture models to estimate abundance and temporal trends of black rhinoceros (*Diceros bicornis* L.) populations from aerial counts. *Glob. Ecol. Conserv.* 19, e00687. <https://doi.org/10.1016/j.gecco.2019.e00687>.
- Kortmann, M., Heurich, M., Latifi, H., Rösner, S., Seidl, R., Müller, J., Thom, S., 2018. Forest structure following natural disturbances and early succession provides habitat for two avian flagship species, capercaillie (*Tetrao urogallus*) and hazel grouse (*Tetrastes bonasia*). *Biol. Conserv.* 226, 81–91. <https://doi.org/10.1016/j.biocon.2018.07.014>.
- Leclercq, B., 1987. *Ecologie et dynamique de population du grand tétras (Tetrao urogallus major L.) dans le Jura français. Université de Dijon*.
- Leclercq, B., Menoni, E., 2018. *Le grand Tétrás*.
- McCaffery, R., Nowak, J.J., Lukacs, P.M., 2016. Improved analysis of lek count data using N-mixture models. *J. Wildl. Manag.* 80, 1011–1021. <https://doi.org/10.1002/jwmg.21094>.
- Meredith, M., 2020. *Bayes with JAGS – a tutorial for wildlife researchers. Goodness-of-fit: SCR models [WWW Document]*. (accessed 8.8.21) [https://mmeredith.net/blog/2020/GOF\\_2.htm](https://mmeredith.net/blog/2020/GOF_2.htm).
- Ministerio para la Transición Ecológica, 2018. Orden TEC/1078/2018, de 28 de septiembre, por la que se declara la situación crítica de *Cistus heterophyllus carthaginensis*, *Lanius minor*, *Margaritifera auricularia*, *Marmarometta angustirostris*, *Mustela lutreola*, *Pinna nobilis* y *Tetrao urogallus* [WWW Document]. <https://www.boe.es/eli/es/o/2018/09/28/tec1078/dof/spa/pdf>.
- Mollet, P., Kéry, M., Gardner, B., Pasinelli, G., Royle, J.A., 2015. Estimating population size for capercaillie (*Tetrao urogallus* L.) with spatial capture-recapture models based on genotypes from one field sample. *PLoS One* 10, 129020. <https://doi.org/10.1371/journal.pone.0129020>.
- Morán-Luis, M., Fameli, A., Blanco-Fontao, B., Fernández-Gil, A., Rodríguez-Muñoz, R., Quevedo, M., Mirol, P., Bañuelos, M.J., 2014. Demographic status and genetic tagging of endangered capercaillie in NW Spain. *PLoS One* 9, 1–9. <https://doi.org/10.1371/journal.pone.0099799>.
- Moreno-Opo, R., Afonso, I., Jiménez, J., Fernández-Olalla, M., Canut, J., García-Ferré, D., Piqué, J., García, F., Roig, J., Muñoz-Igualada, J., González, L.M., López-Bao, J.V., 2015. Is it necessary managing carnivores to reverse the decline of endangered prey species? Insights from a removal experiment of mesocarnivores to benefit demographic parameters of the pyrenean capercaillie. *PLoS One* 10, 1–17. <https://doi.org/10.1371/journal.pone.0139837>.
- Moss, R., Picozzi, N., Summers, R.W., Baines, D., 2000. Capercaillie *Tetrao urogallus* in Scotland- demography of a declining population. *Ibis (Lond. 1859)* 142, 259–267. <https://doi.org/10.1111/j.1474-919X.2000.tb04865.x>.
- Moss, R., Oswald, J., Baines, D., 2001. Climate change and breeding success: decline of the capercaillie in Scotland. *J. Anim. Ecol.* 70, 47–61. <https://doi.org/10.1046/j.1365-2656.2001.00473.x>.
- NIMBLE Development Team, 2019. *NIMBLE User Manual 164*.
- Peakall, R., Smouse, P.E., 2006. GENALEX 6: genetic analysis in excel. Population genetic software for teaching and research. *Mol. Ecol. Notes* 6, 288–295. <https://doi.org/10.1111/j.1471-8286.2005.01155.x>.
- Pérez, T., Vázquez, J.F., Quirós, F., Domínguez, A., 2011. Improving non-invasive genotyping in capercaillie (*Tetrao urogallus*): redesigning sexing and microsatellite primers to increase efficiency on faeces samples. *Conserv. Genet. Resour.* 3, 483–487. <https://doi.org/10.1007/s12686-011-9385-8>.
- Péron, G., Garel, M., 2019. Analyzing patterns in population dynamics using repeated population surveys with three types of detection data. *Ecol. Indic.* 106, 105546. <https://doi.org/10.1016/j.ecolind.2019.105546>.
- Péron, G., Nicolai, C.A., Koons, D.N., 2012. Demographic response to perturbations: the role of compensatory density dependence in a north american duck under variable harvest regulations and changing habitat. *J. Anim. Ecol.* 81, 960–969. <https://doi.org/10.1111/j.1365-2656.2012.01980.x>.
- Picozzi, N., Moss, R., Catt, D.C., 1996. Capercaillie habitat, diet and management in a Sitka spruce plantation in Central Scotland. *Forestry* 69, 372–388. <https://doi.org/10.1093/forestry/69.4.373>.
- Piertney, S.B., Dallas, J.F., 1997. Isolation and characterization of hypervariable microsatellites in the red grouse *Lagopus lagopus scoticus*. *Mol. Ecol.* 6, 93–95. <https://doi.org/10.1046/j.1365-294X.1997.00154.x>.
- Piertney, S.B., Höglund, J., 2001. Polymorphic microsatellite DNA markers in black grouse (*Tetrao tetrix*). *Mol. Ecol. Notes* 1, 303–304. <https://doi.org/10.1046/j.1471-8278.2001.00118.x>.
- Piggott, M.P., Bellemain, E., Taberlet, P., Taylor, A.C., 2004. A multiplex pre-amplification method that significantly improves microsatellite amplification and error rates for faecal DNA in limiting conditions. *Conserv. Genet.* 5, 417–420. <https://doi.org/10.1023/B:COGE.0000031138.67958.44>.
- Pollo, C.J., Robles, L., Seijas, J.M., García-Miranda, A., Otero, R., 2003. Cantabrian capercaillie *Tetrao urogallus cantabricus* population size and range trend. Will the capercaillie survive in the Cantabrian Mountains? *Grouse News* 26, 3–5.
- Pollo, C.J., Robles, L., Seijas, J.M., García-Miranda, Á., Otero, R., 2005. Trends in the abundance of cantabrian capercaillie *Tetrao urogallus cantabricus* at leks on the southern slope of the cantabrian mountains, north-West Spain. *Bird Conserv. Int.* 15, 397–409. <https://doi.org/10.1017/S0959270905000626>.
- Quevedo, M., Bañuelos, M.J., Sáez, O., Obeso, J.R., 2006. Habitat selection by cantabrian capercaillie *Tetrao urogallus cantabricus* at the edge of the species' distribution. *Wildlife Biol.* 3, 267–276.
- R Core Team, 2020. *R: A language and environment for statistical computing. R Found. Stat. Comput.*
- Rajala, P., 1974. The structure and reproduction of finnish populations of capercaillie *Tetrao urogallus* and black grouse *Tetrao tetrix*. on the basis of late summer census data from 1963–1966.
- Rodríguez-Muñoz, R., Mirol, P.M., Segelbacher, G., Fernández, A., Tregenza, T., 2007. Genetic differentiation of an endangered capercaillie (*Tetrao urogallus*) population at the southern edge of the species range. *Conserv. Genet.* 8, 659–670. <https://doi.org/10.1007/s10592-006-9212-z>.
- Royle, J.A., 2004. N-mixture models for estimating population size from spatially replicated counts. *Biometrics* 60, 108–115. <https://doi.org/10.1111/j.0006-341X.2004.00142.x>.
- Royle, J.A., Dorazio, R.M., Link, W.A., 2007. Analysis of multinomial models with unknown index using data augmentation. *J. Comput. Graph. Stat.* 16, 67–85. <https://doi.org/10.1198/106186007X181425>.
- Royle, J.A., Nichols, J.D., Karanth, K.U., Gopalaswamy, A.M., 2009. A hierarchical model for estimating density in camera-trap studies. *J. Appl. Ecol.* 46, 118–127. <https://doi.org/10.1111/j.1365-2664.2007.0>.
- Royle, J.A., Chandler, R.B., Sollmann, R., Gardner, B., 2014. *Spatial capture-recapture. Elsevier, Academic Press, Waltham, Massachusetts* <https://doi.org/10.1016/B978-0-12-405939-9.00026-8>.
- Santorek, A., Zwijacz-Kozica, T., Dulisz, B., Merta, D., Rutkowski, R., 2021. Biased sex-ratio in woodland grouse population of the Tatra National Park, suggested by molecular sexing of non-invasive samples. *Fragm. Faun.* 63, 129–136. <https://doi.org/10.3161/00159301FF2020.63.2.129>.
- Schaub, M., Kéry, M., 2022. *Integrated Population Models: Theory and Ecological Applications with R and JAGS. First Edit. Elsevier*.
- Segelbacher, G., Paxton, R.J., Steinbrück, G., Trontelj, P., Storch, I., 2000. Characterization of microsatellites in capercaillie *Tetrao urogallus* (AVES). *Mol. Ecol.* 9, 1934–1935.
- Storch, I., 1997. Male territoriality, female range use, and spatial organization of capercaillie *Tetrao urogallus* leks. *Wildlife Biol.* 3, 149–161. <https://doi.org/10.2981/wlb.1997.019>.
- Storch, I., Bañuelos, M.J., Fernández-Gil, A., Obeso, J.R., Quevedo, M., Rodríguez-Muñoz, R., 2006. Subspecies cantabrian capercaillie *Tetrao urogallus cantabricus* endangered according to IUCN criteria. *J. Ornithol.* 147, 653–655. <https://doi.org/10.1007/s10336-006-0101-5>.
- Summers, R.W., Willi, J., Selvidge, J., 2009. Capercaillie *Tetrao urogallus* nest loss and attendance at abernethy Forest Scotland. *Wildl. Biol.* 15, 319–327. <https://doi.org/10.2981/08-036>.
- Tobajas, J., Oliva-Vidal, P., Piqué, J., Afonso-Jordana, I., García-Ferré, D., Moreno-Opo, R., Margalida, A., 2021. Scavenging patterns of generalist predators in forested areas: the potential implications of increase in carrion availability on a threatened capercaillie population. *Anim. Conserv.* <https://doi.org/10.1111/acv.12735>.
- Valière, N., 2002. GIMLET: a computer program for analysing genetic individual identification data. *Mol. Ecol. Notes* 2, 377–379. <https://doi.org/10.1046/j.1471-8278.2002.00228.x>.
- Vázquez, J.F., Pérez, T., Albornoz, J., Domínguez, A., 2013. Census and effective population size of the endangered cantabrian capercaillie (*Tetrao urogallus*) estimated from non-invasive samples. *Grouse News* 46, 12–26.
- Vehtari, A., Gelman, A., Simpson, D., Carpenter, B., Bürkner, P.-C., 2020. Rank-normalization, folding, and localization: an improved R for assessing convergence of MCMC (with Discussion). *Bayesian Anal.* 16, 667–718. <https://doi.org/10.1214/20-ba1221>.
- Watanabe, S., 2013. A widely applicable bayesian information criterion. *J. Mach. Learn. Res.* 14, 867–897.
- Williams, B.K., Nichols, J.D., Conroy, M.J., 2002. *Analysis and management of animal populations. Academic Press/Elsevier, San Diego, U.S.A.*
- Zhao, Q., Heath-Acre, K., Collins, D., Conway, W., Weegman, M.D., 2021. Integrated population modelling reveals potential drivers of demography from partially aligned data: a case study of snowy plover declines under human stressors. *PeerJ* 9, 1–24. <https://doi.org/10.7717/peerj.12475>.
- Zipkin, E.F., Thorson, J.T., See, K., Lynch, H.J., Grant, E.H.C., Kanno, Y., Chandler, R.B., Letcher, B.H., Royle, J.A., 2014. Modeling structured population dynamics using data from unmarked individuals. *Ecology* 95, 22–29. <https://doi.org/10.1890/13-1131.1>.